Polymer 51 (2010) 2033–2039

Contents lists available at ScienceDirect

Polymer

journal homepage: www.elsevier.com/locate/polymer

Characterization of the adhesion of single-walled carbon nanotubes in poly (p-phenylene terephthalamide) composite fibres

Libo Deng [a], Robert J. Young [a,*], Sybrand van der Zwaag [b], Steven Picken [c]

[a] Materials Science Centre, School of Materials, University of Manchester, Manchester M1 7HS, UK
[b] Faculty of Aerospace Engineering, Delft University of Technology, 2629 HS, Delft, The Netherlands
[c] Department of Chemical Technology, Delft University of Technology, 2628 BS Delft, The Netherlands

ARTICLE INFO

Article history:
Received 21 December 2009
Received in revised form
22 February 2010
Accepted 22 February 2010
Available online 1 March 2010

Keywords:
Aramids
Carbon nanotubes
Raman spectroscopy

ABSTRACT

Poly(p-phenylene terephthalamide)/single-walled carbon (PPTA/SWNT) composite fibres with different draw ratios have been spun using a dry-jet wet spinning process and their structure and deformation behaviour analysed using Raman spectroscopy. The dispersion of nanotube has been examined by Raman scattering intensity mapping along the fibre. The nanotubes improved the polymer orientation in composite fibre with a draw ratio of 2 but degraded the orientation at higher draw ratios. The mechanical reinforcing effect by nanotubes is related to the change of polymer orientation, suggesting a dominant role of polymer orientation in mechanical performance of the composite fibre. High efficiency of stress transfer within the strain range of 0–0.35% and breakdown of the interface at higher strains has been found in the composite fibres through an in situ Raman spectroscopic study during fibre deformation. Cyclic loading applied on the fibre has indicated reversible deformation behaviour at low strain and gradual damage of the interface at high strains.

1. Introduction

Poly(p-phenyleneterephthalamide) (PPTA) fibres, which are made up of oriented bundles of rig-rod polymer molecules, are characterized by high stiffness and tensile strength. For commercial PPTA fibres such as Twaron and Kevlar fibres, however, there is still a gap between the actual modulus (140 GPa) and the crystallite modulus (200 GPa) measured with X-ray diffraction [1,2]. It is desirable but great challenge to enhance the high performance PPTA fibres.

Carbon nanotubes (CNTs) are now believed to be the ultimate reinforcing filler for polymers due to their extraordinary mechanical properties [3,4]. They have shown mechanical reinforcement in a variety of polymers such as epoxy [5], PVA [6], PMMA [7] and polyamide [8] with very few successful examples on high performance polymers [9]. More recently, Coleman's group have reported [10] a significant improvement in mechanical properties of Kevlar fibres by incorporating multi-walled carbon nanotubes, in which the Kevlar/nanotube composite fibres were prepared by swelling of Kevlar fibre in a suspension of nanotubes in the solvent N-methylpyrrolidone. Although the conventional dry-jet wet spinning process for preparation of PPTA fibre is believed to be feasible and is suitable for the mass-production of PPTA/NT composite fibres, little work has been published so far. In this present study, we investigate the effect of nanotubes on PPTA/SWNT composite fibres spun with a dry-jet wet spinning process by using Raman spectroscopy, which has proved to be a powerful technique in studying CNT based polymer composites. We demonstrate here that important issues involved in mechanical reinforcement, such as the state of dispersion and orientation of nanotubes, and the interfacial stress transfer can be assessed using Raman spectroscopy [11].

2. Experimental

2.1. Materials

The neat PPTA and PPTA/SWNT composite fibres were spun with a dry-jet wet spinning process. Fibres with different draw ratios (DRs), which is defined as the ratio of fibre take-up speed and dope extruding speed, have been spun to understand the influence of processing conditions on the properties of the fibres. The nanotubes in the composite fibres were pristine HiPco SWNTs, and the content of nanotubes was 0.5% by weight for all composite fibres.

2.2. Mechanical testing

Single-fibres of PPTA and PPTA/SWNT were mounted across a cardboard window with a gauge length of 50 mm. Both ends of

* Corresponding author. Tel.: +44 161 306 3550.
E-mail address: robert.young@manchester.ac.uk (R.J. Young).

0032-3861/$ – see front matter © 2010 Elsevier Ltd. All rights reserved.
doi:10.1016/j.polymer.2010.02.040

the fibre were fixed using quick-setting epoxy resin to achieve good adhesion and prevent slippage of fibres during mechanical testing. The samples were left in the mechanical testing room, in which the temperature was set constantly at 23 ± 0.1 °C and humidity at 50 ± 5%, for at least 48 h prior to mechanical testing. The tensile testing was carried out using an Instron-1122 universal testing machine. The machine was equipped with a 1 N load cell and the crosshead speed was set at 0.5 mm/min. The sample was carefully mounted onto the testing machine to ensure the fibre axis was parallel to the loading axis. Both sides of the paper frame were then burned away prior to mechanical testing. The fibre diameter was measured using a Philips XL30 FEG SEM, which was operated at an accelerating voltage of 5 kV. A minimum of 20 specimens for each type of fibre were tested for statistical accuracy.

2.3. Raman spectroscopy

Raman spectra were obtained using a Renishaw 1000 system with a He–Ne laser. The laser spot size was about 2 μm, and the power was about 1 mW when the laser is focused on the fibre. The curves were fitted using a Lorentzian function. For single-fibre deformation test, a custom-made tensile rig was used for stretching the paper card on which the fibre was mounted. The strain was recorded using a micrometer which is attached to the rig, and the force applied on the fibre was recorded using a transducer. Raman spectra were taken at each strain level.

3. Results and discussion

3.1. Composite fibre structure

Fig. 1 shows the Raman spectrum of neat PPTA fibre, the original SWNTs and PPTA/SWNT composite fibre. Characteristic bands of both nanotubes and PPTA polymers can be seen from the composite fibres, and this enables the use of Raman spectroscopy for further characterization. Two features have been found by comparing the spectrum of composite and the original SWNTs: 1) The G′-band from the composite fibre is higher in wavenumber than that from the original SWNTs in air, and fibres with higher DRs show a higher peak position, indicating residual compressive stress in the fibre upon drawing; and 2) The multiple peaks observed in the low-frequency region (radial breathing mode, RBM), together with the peak position and bandwidth of G′-band suggest the nanotubes were still in bundles even the processing condition has been optimized to exfoliate nanotubes.

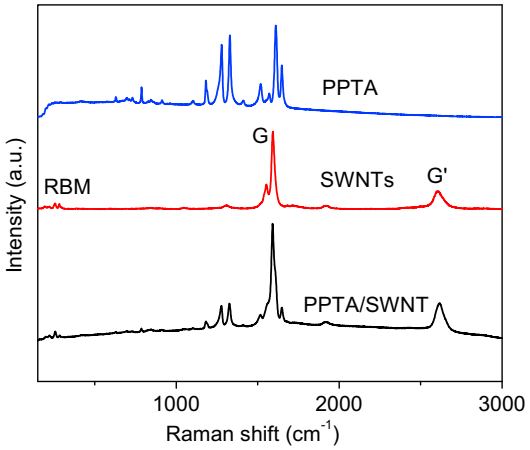

Fig. 1. Raman spectrum of neat PPTA, SWNTs and PPTA/SWNT composite fibre.

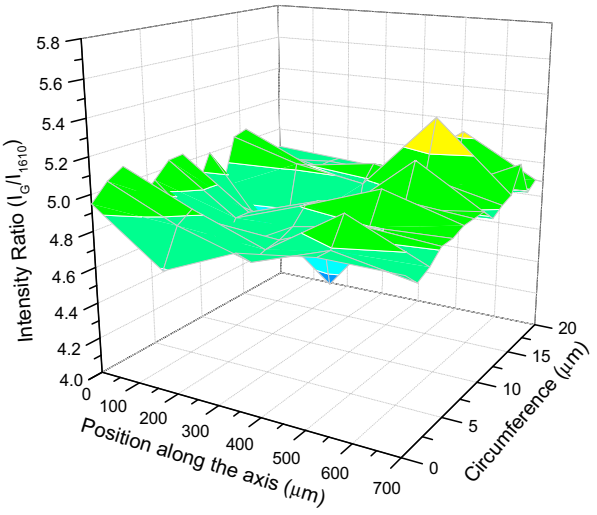

Fig. 2. Intensity ratio of nanotube G-band to PPTA 1610 cm^{-1} band along a PPTA/SWNT fibre with a DR of 2, showing the uniform distribution of SWNTs.

To examine the distribution of nanotube bundles, Raman intensity mapping was undertaken by scanning the laser over the fibre surface. The relative intensity of nanotube G-band to PPTA 1610 cm^{-1} band (I_G/I_{1610}) is found to be uniform at different positions along the fibre (Fig. 2), which reveals that the nanotube bundles were well dispersed on the micrometer scale. The state of dispersion was found to be independent of the fibre draw ratio.

The orientation of both the nanotubes and the polymer molecules can be characterized using polarized Raman spectroscopy. For perfectly aligned nanotubes or polymer chains, when using a VV configuration where the incident and scattered laser are both parallel to the sample axis (Fig. 3), the dependence of Raman intensity I^{VV}_{Fibre} upon the angle β is found to be [12,13]:

$$I^{VV}_{Fibre} \propto \cos^4 \beta \tag{1}$$

For a sample consisting of nanotubes distributed over a range of angles, the Raman intensity is a sum of contributions from all nanotubes, and can be written as [14,15]:

$$I^{VV}_{Fibre}(\varphi) \propto \left(\cos^4 \varphi - \frac{6}{7}\cos^2 \varphi + \frac{3}{35}\right)\langle P_4(\cos\beta)\rangle + \left(\frac{6}{7}\cos^2 \varphi - \frac{2}{7}\right)\langle P_2(\cos\beta)\rangle + \frac{1}{5} \tag{2}$$

where φ is the angle between laser polarization and fibre axis, β is the angle between laser polarization and nanotube axis, and $\langle P_2(\cos\beta)\rangle$ and $\langle P_4(\cos\beta)\rangle$ are the orientation order parameters. The parameter $\langle P_2(\cos\beta)\rangle$ is more important for axial symmetric materials and is also known as the Herman's orientation factor, with its value of 1 for perfect alignment and 0 for a random distribution [15]. To determine the polymer orientation quantitatively, either the Raman intensity at different angles (for a complete procedure [16]) or the depolarization ratio coupled with the intensity at different configuration of laser polarization (for

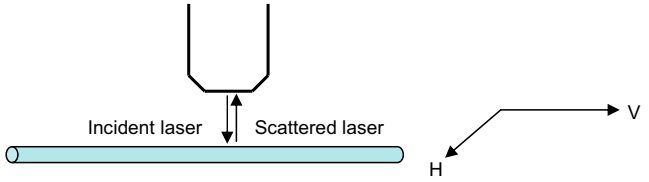

Fig. 3. Schematic diagram of the configuration of the laser polarization.

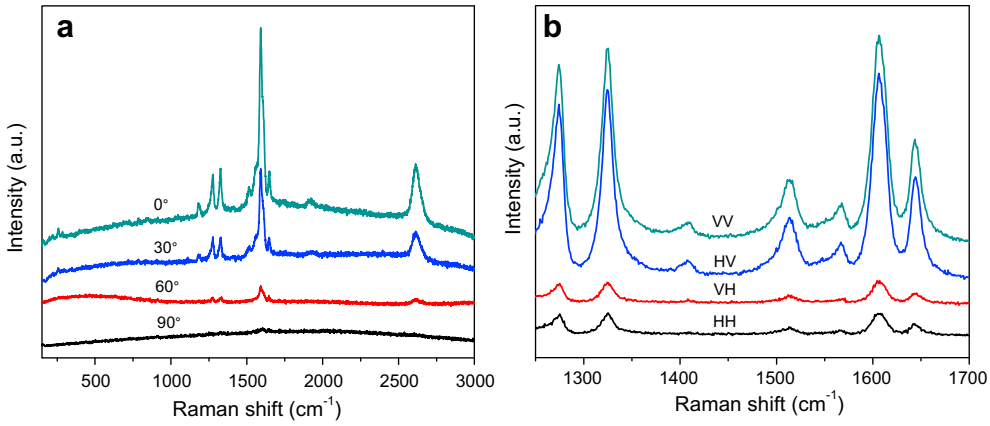

Fig. 4. Raman spectra of a) composite fibre at different angles (VV configuration) and b) neat fibre at different configurations. The DR is 11 for both fibres.

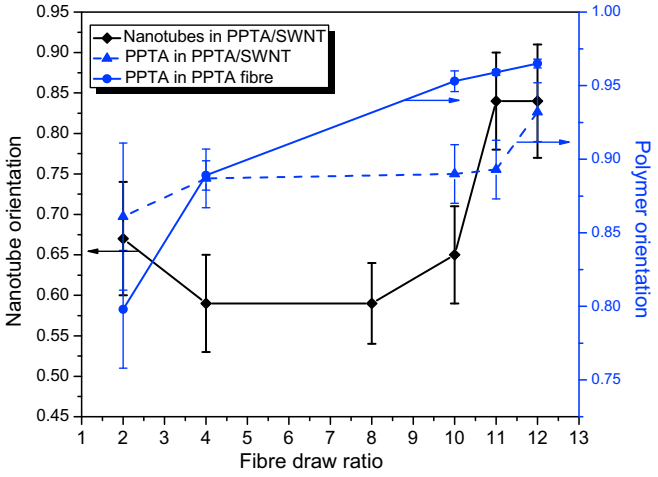

Fig. 5. Degree of alignment of nanotubes and polymers in the PPTA/SWNT composite and neat PPTA fibres with different DRs.

a simplified model [17]) is required. Here a qualitative parameter $P = 1 - I_{HH}/I_{VV}$ is employed to characterize the orientation as the depolarization ratio for isotropic PPTA polymer is not available and this qualitative parameter has proved to be a simple yet effective way to assess the relative molecular orientation of polymers that possess the same structure [17].

Fig. 4 shows the Raman spectra of a composite fibre at different angles with respect to the laser polarization, and the spectra of the neat PPTA fibre at different configurations. The dramatic decease of the intensity with the increasing angle and the difference at different laser polarization indicates that both the nanotubes and polymer molecules are aligned parallel to the fibre axis.

The orientation parameter $\langle P_2(\cos\beta)\rangle$ for the nanotubes and the qualitative orientation parameter P for PPTA are plotted as a function of fibre draw ratio as shown in Fig. 5. The large standard deviation in the orientation parameter for nanotubes is due to probing different areas while rotating the sample. It can be seen the orientation of both the nanotubes and polymer molecules generally increases with the DR of the fibre. Compared to the neat fibre, the orientation of polymer has only been improved for the composite fibre with a DR of 2; and for fibres with higher DRs the polymer molecules are better oriented in the neat fibres than in the composite fibres. This may be very important for the mechanical performance of the fibre. It remains unclear at this stage how nanotubes influence the arrangement of the polymer chains in the composite fibre.

3.2. Mechanical properties

Mechanical properties have been measured with an Instron machine and the typical stress–strain curves for neat PPTA and PPTA/SWNT fibres are shown in Fig. 6. It can be seen the slope in these curves decreases when the strain exceeds 0.5% and increases after 1%. The variation in modulus is thought to be due to change of the molecular configuration under strain and the variation becomes less pronounced as the DR of fibres increases. The mechanical parameters are plotted as a function of DR in Fig. 7. The dependence of the modulus on DR for unreinforced PPTA fibres as

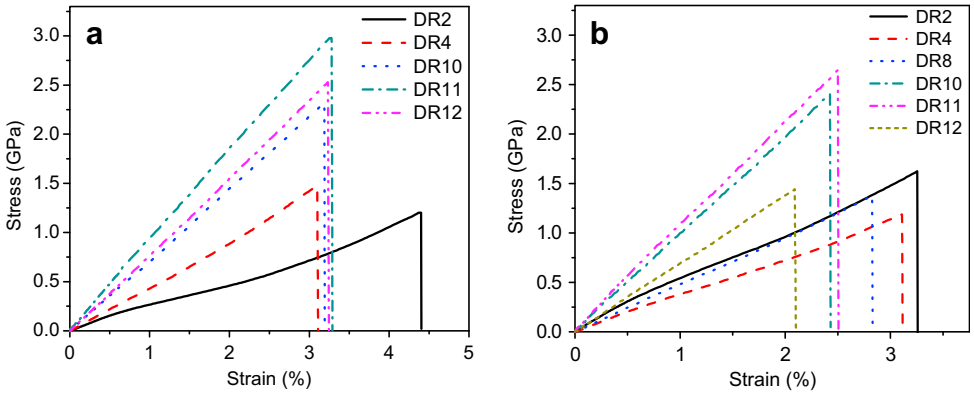

Fig. 6. Typical stress–strain curves of a) PPTA fibres and b) PPTA/SWNT fibres.

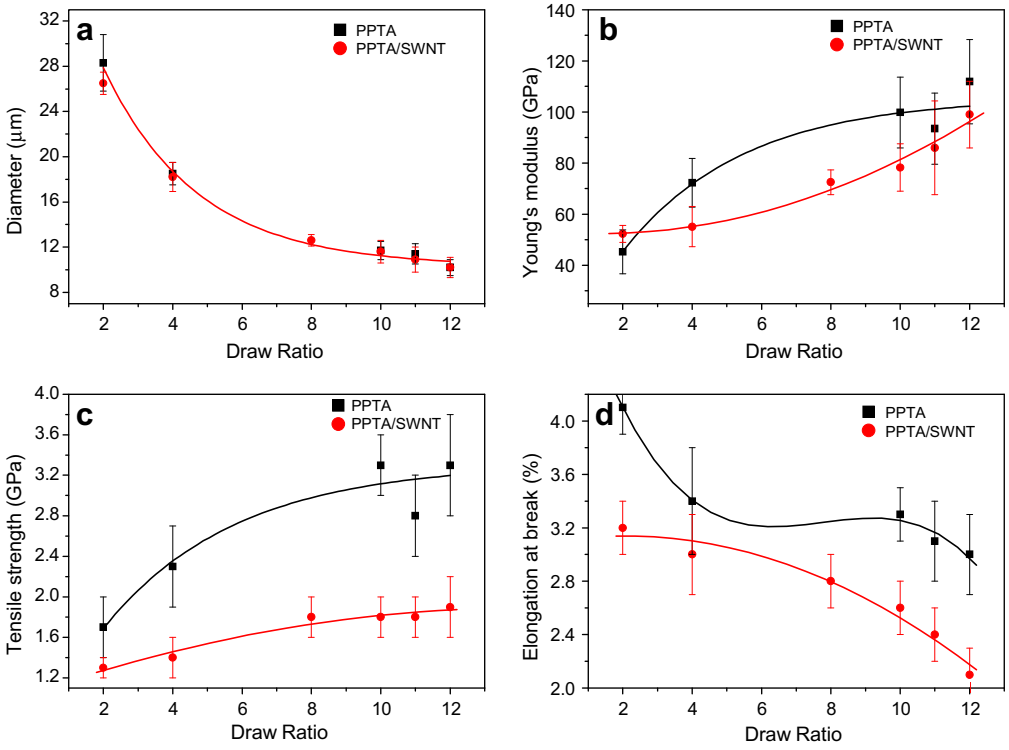

Fig. 7. Mechanical properties of PPTA fibres and PPTA/SWNT fibres.

a function of polymer spindope concentration and coagulation conditions has been explained quantitatively elsewhere [18]. It is found that the Young's modulus of reinforced fibres has been improved by 15% for composite fibre relative to the neat fibre with a DR of 2. For fibres with higher DRs, the mechanical properties are degraded, an effect that has been observed for other high performance polymer/nanotube composites as well. It should be noted that mechanical reinforcement of polymers by nanotubes have been mostly on relatively low modulus polymers so far, and mechanical degradation by pristine nanotubes has also been reported where poor dispersion of nanotubes and weak interfacial interactions occur [19–22].

Consider the mechanical reinforcing of PPTA by SWNTs firstly based on the simple rule of mixtures:

$$E_c = V_{NT}E_{NT} + (1 - V_{NT})E_m \quad (3)$$

where E_c, E_{NT}, and E_m are the modulus of the composite fibre, SWNTs, and neat PPTA, respectively; and V_{NT} is the volume fraction of SWNTs and is taken as 0.5% in PPTA/SWNT fibre. The modulus of neat PPTA fibre is taken as 100 GPa as indicated by mechanical testing (e.g. DR = 11). It has been found the modulus of SWNT bundles decreases rapidly as the rope diameter increases [23]. For example, the modulus of a SWNT rope with a diameter of 13.5 nm drops to 150 GPa. Substituting these values into Equation (3) gives approximately only 1% improvement in modulus of the PPTA fibre for the CNT concentration employed here.

Another factor that can significantly influence the mechanical performance of the materials is the orientation of the structural units. In fact, it is the rigid rod-like polymer chain, coupled with high crystallinity and high orientation that impart PPTA fibres with high modulus and tensile strength. A comparison of Fig. 5 with Fig. 6b reveals that the Young's modulus improves when the nanotubes improve the orientation of polymers with respect to the neat fibre and reduces when the orientation of polymer deteriorates. This indicates that the orientation of polymer plays a dominant role in mechanical performance of these composite fibres.

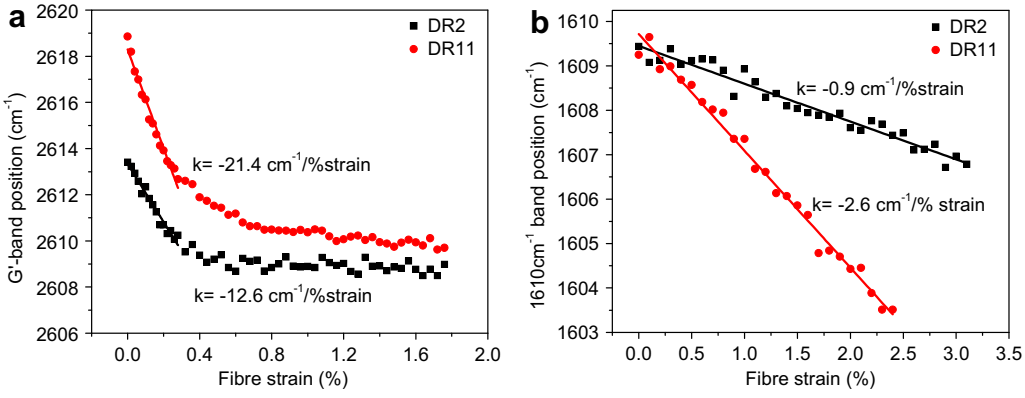

Fig. 8. Variation of Raman band peak position for composite fibre with different DRs under tensile deformation: a) nanotube G′-band and b) PPTA 1610 cm^{-1} peak.

Table 1
Nanotube G′-band shift rate and the final shift in different composites.

Polymer	CNT type	Functionalization	Shift rate (cm^{-1}/%strain)	Maximum shift (cm^{-1})	Reference
PVA	Elicarb	Pristine	3.7	~7	[28]
		–COOH	5.6	~8	
PVA	HiPco	Pristine	17	~7	Unpublished
Epoxy	HiPco	Pristine	13	8	[29]
Polystyrene		Annealed	~9.5	7	[27]
Polycarbonate	Undiym Inc	Pristine	6	2.6	[30]
		PCA-functionalized	8.5	4	
PMMA	HiPco	Pristine	15	4	[31]
PPTA DR2	HiPco	Pristine	12.5	4	This work
PPTA–DR11	HiPco	Pristine	23	8	This work

3.3. Interfacial effects

In situ Raman spectroscopy was employed to follow the deformation behaviour of the composite fibres. Fig. 8 shows the variation of Raman band position during tensile deformation. The PPTA 1610 cm^{-1} peak shifted to lower wavenumber monotonically with increasing strain up to fibre fracture. On the other hand, the nanotube G′-band and G-band wavenumber were found to decrease as the strain increased until it reached 0.35%, and the down shift for both bands ceased when the strain exceeded 0.6%. This indicates breakdown of the interface in the strain range of 0.35–0.6%, which can be a result of interfacial sliding at NT–NT interface and/or NT-polymer interface [24].

The Raman shift rate increases with the DR of the fibre, and is found to scale with the modulus of the composite fibre. The large band shift rate of nanotube G′-band within small strain range is clearly an indication of stress transfer from the matrix to the nanotubes [25]. Molecular dynamics simulation carried out by Yang et al. [26] has demonstrated that strong interfacial adhesion exists between nanotubes and polymers that contain aromatic rings in their backbone, as is the case for PPTA molecules. This strong interfacial interaction should give rise to mechanical reinforcing on PPTA fibres, but is not the case for PPTA/SWNT fibres except for the fibre with a DR of 2. Solokov et al. [27] have also observed the phenomenon that high efficiency of stress transfer results in very limited reinforcement and the reason remained unclear in their work. In our case, the matrix has been degraded compared to the neat PPTA due to the orientation deterioration, which consequently resulted in the negative reinforcing effect in the composite even when good stress transfer has been observed.

The overall down shift of nanotube G′-band in the fibre deformation process reflects the strength of the interface. For fibres with a DR of 11 in which the nanotubes are highly aligned, a maximum down shift of 8 cm^{-1} has been observed. A comparison of nanotube

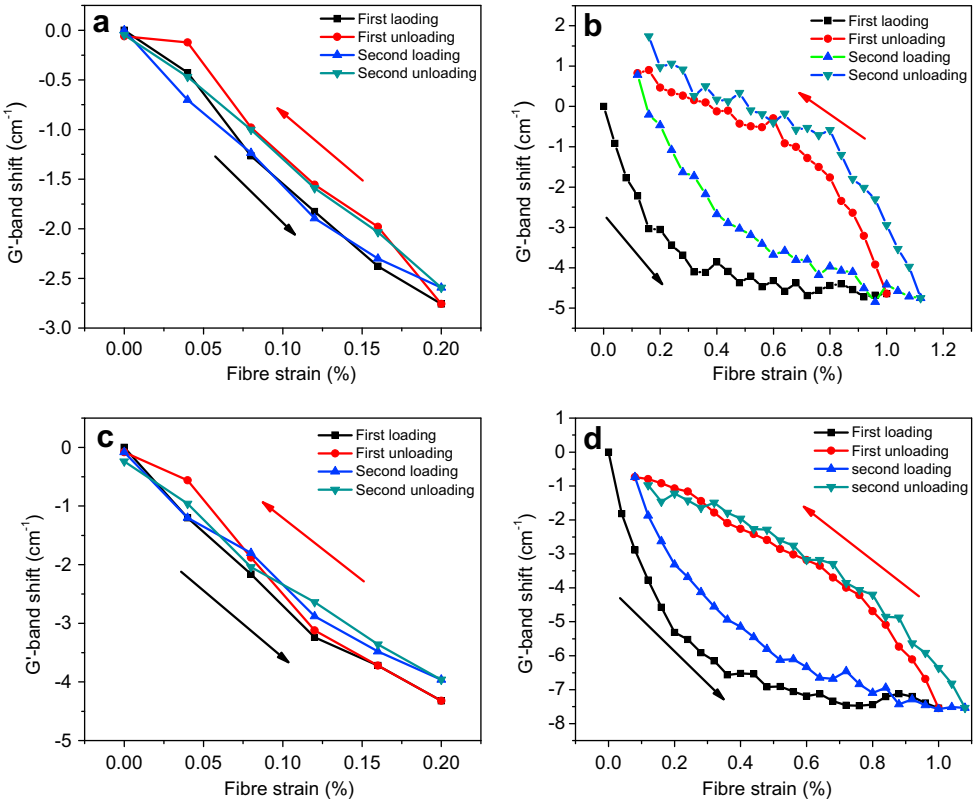

Fig. 9. Variation of G′-band under cyclic loading for PPTA/SWNT fibres: (a) and (b), DR = 2; and (c) and (d), DR = 11.

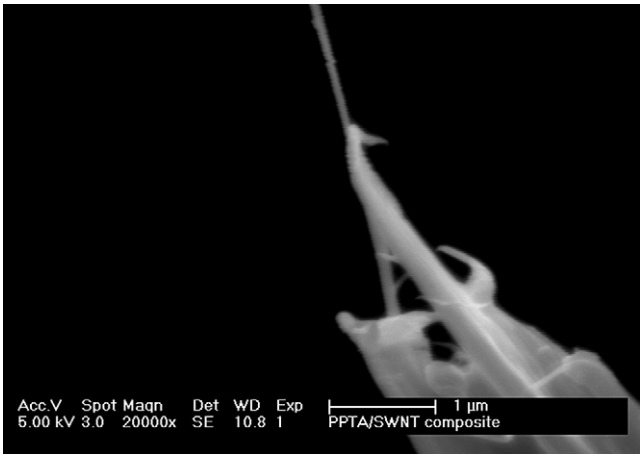

Fig. 10. SEM image of the fracture surface of a PPTA/SWNT fibre with a DR of 2.

G′-band shift rates together with the final down shifts that have been reported in the literature is listed in Table 1. It is difficult to compare the shift rate for different composites system as it depends on the orientation and type (preparation method) of nanotubes, as well as the properties of polymer matrix. However, despite the significant variation in Raman shift rate observed in different composites, the maximum final down shift of nanotube G′-band is comparable, indicating a similar interfacial strength in these non-covalently bonded nanocomposites.

The reversibility of deformation of the composite fibre was investigated by loading and unloading on the sample to different strain levels. Two cycles of loading were applied at each strain level and the G′-band response are shown in Fig. 9. In the cyclic loading within the strain range of 0.2% (Fig. 9a and c), G′-band goes upwards in the unloading process following nearly the same path as the loading line, and the curve for the second cycle overlaps with the first one, indicating a reversible deformation process [31]. When the strain recovers back from 1% where most interfacial sliding has been activated, the G′-band returns in a different path such that hysteresis is observed. For fibres with a DR of 2, the shift rate in the initial stage of the unloading curve is similar to the loading curve, and the second cycle begins with a slightly smaller shift rate showing somewhat reversible behaviour. All these suggest that breakdown of the interface is a gradual process. While for fibres with a higher DR (Fig. 9d), the Raman shift rate upon unloading and in the second loading cycle is smaller compared to the first loading curve, which the interfacial failure in the first cycle is more significant in this fibre and the interfacial interaction is weaker compared to the fibre with a DR of 2.

After being fully unloaded from 1% strain, the G′-band in composite fibre with a DR of 2 is about 1.7 cm^{-1} higher than the initial position prior to cyclic loading (Fig. 9b), suggesting 0.34 GPa of residual compressive stress upon unloading, based on the calibration for carbon fibres of -5 cm^{-1}/GPa [29]. This residual stress is thought to arise from the friction between the mismatched nanotube and matrix. In addition, the interfacial sliding results in approximately 0.84 MJ/m^3 of energy dissipated (calculated from the area of the loop between loading and unloading stress–strain curve [32]) in the loading–unloading cycle, which is 50% higher than in the neat PPTA fibre. An SEM image of the fracture surface of a composite fibre showed that rigid SWNT ropes with a diameter of 30–70 nm have been pulled out from the matrix (Fig. 10). Therefore, the nanotube-polymer sliding is likely responsible for the increase in energy dissipation in the composite fibre.

While the energy dissipation related to the CNT debonding and sliding during cyclic straining for strains between 0.3% and 1.0% has been clearly demonstrated here, it is interesting to note that the critical strain for debonding coincides with the strain at which yielding in unreinforced PPTA fibres occurs [33]. It is not to be excluded that the yielding of the PPTA structure itself plays a role in the debonding conditions, but more research is required to establish such a relation.

4. Conclusions

PPTA/SWNT composite fibres spun with a dry-jet wet spinning process have been characterized using Raman spectroscopy. Relative intensity of nanotube G-band and PPTA 1610 cm^{-1} peak showed a good dispersion of nanotubes in the composite fibre. The nanotubes improved the orientation of polymer in the composite fibre with a DR of 2 but degraded the orientation for higher DRs. This change of polymer orientation is thought to have direct effect on the efficiency of mechanical reinforcement of the PPTA fibre, showing the dominant role of polymer orientation upon mechanical performance of the composite fibres. An in situ Raman spectroscopy study during fibre deformation revealed good stress transfer from the matrix to nanotubes in low strain range, and the interface failed when the strain exceeded 0.3–0.5% depending on the initial orientation of the fibre. Cyclic loading has indicated reversible deformation within the strain range of 0–0.2% and a gradual breakdown of the interface at higher strains. The frictional sliding in the composite fibres results in improved energy dissipation and this may be useful in structural damping applications [34,35].

Acknowledgements

One of the authors (L.D.) would like to thank the Chinese and UK governments for financial support through the “China/UK Scholarship for excellence” scheme.

References

[1] Yeh WY, Young RJ. Polymer 1999;40:857.
[2] Northolt MG. Polymer 1980;21:1199.
[3] Coleman J, Khan U, Blau W, Gun'Ko Y. Carbon 2006;44:1624.
[4] Coleman J, Khan U, Gun'Ko Y. Adv Mater 2006;18:689.
[5] Zhu J, Peng H, Rodriguez-Macias F, Margrave JL, Khabashesku VN, Imam AM, et al. Adv Funct Mater 2004;14:643.
[6] Coleman J, Cadek M, Blake R, Nicolosi V, Ryan K, Belton C, et al. Adv Funct Mater 2004;14:791.
[7] Blond D, Barron V, Ruether M, Ryan KP, Nicolosi V, Blau WJ, et al. Adv Funct Mater 2006;16:1608.
[8] Sandler JKW, Pegel S, Cadek M, Gojny F, Es Mv, Lohmar J, et al. Polymer 2004;45:2001.
[9] Kumar S, Dang T, Arnold F, Bhattacharyya A, Min B, Zhang X, et al. Macromolecules 2002;35:9039.
[10] O'Connor I, Hayden H, Coleman J, Gun'ko Y. Small 2009;5:466.
[11] Zhao Q, Wagner HD. Phil Trans R Soc Lond A 2004;362:2407.
[12] Gommans H, Alldredge J, Tashiro H, Park J, Magnuson JJ. Appl Phys 2000;88:2509.
[13] Hwang J, Gommans H, Ugawa A, Tashiro H, Haggenmueller R, Winey K, et al. Phys Rev B 2000;62:R13310.
[14] Liu T, Kumar S. Chem Phys Lett 2003;378:257.
[15] Pérez R, Banda S, Ounaiesa ZJ. Appl Phys 2008;103:074302.
[16] Bower DIJ. Polym Sci B 1972;10:2135.
[17] Frisk S, Ikeda RM, Chase DB, Rabolt JF. Appl Spectrosc 2004;58:279.
[18] Picken SJ, van der Zwaag S, Northolt MG. Polymer 1992;33:2998.
[19] Ajayan P, Schadler L, Giannaris C, Rubio A. Adv Mater 2000;12:750.
[20] Bhattacharyy A, Sreekumar T, Liu T, Kmar S, Errison L, Haug R, et al. Polymer 2003;44:2373.
[21] Manchadoa M, Valentinib L, Biagiottib J, Kennyb JM. Carbon 2005;43:1499.
[22] Vigolo B, Vincent B, Eschbach J, Bourson P, March J, McRae E, et al. Phys Chem C 2009;113:17648.
[23] Salvetat J, Briggs A, Bonard J, Bacsa R, Kulik A, Stöckli T, et al. Phys Rev Lett 1999;82:944.
[24] Kannan P, Eichhorn SJ, Young RJ. Nanotechnology 2007;18:235707.
[25] Cui S, Kinloch IA, Young RJ, Noé L, Monthioux M. Adv Mater 2009;21:3591.
[26] Yang M, Koutsos V, Zaiser MJ. Phys Chem B 2005;109:10009.

[27] Chang TE, Kisliuk A, Rhodes SM, Brittain WJ, Sokolov AP. Polymer 2006;47:7740.
[28] Lachman N, Bartholome C, Miaudet P, Maugey M, Poulin P, Wagner HJ. Phys Chem C 2009;113:4751.
[29] Cooper C, Young R, Halsall M. Composites: Part A 2001;32:401.
[30] Simmons TJ, Bult J, Hashim DP, Linhardt RJ, Ajayan PM. ACS Nano 2009;3:865.
[31] Mu M, Osswald S, Gogotsi Y, Winey K. Nanotechnology 2009;20:335703.
[32] Kao C, Young RJ. J Mater Sci 2010;45:1425.
[33] Northolt MG, Baltussen JJM, Schaffers-Korff B. Polymer 1995;36:348.
[34] Koratkar N, Suhr J, Joshi A, Kane R, Schadler L, Ajayan P, et al. Appl Phys Lett 2005;87:063102.
[35] Suhr J, Koratkar N, Keblinski P, Ajayan P. Nat Mater 2005;4:134.